DOI: 10.1002/ejic.200701299

N-Phosphanylformamidines (phosfam) $R_2'N–C(H)=N–PR_2$: One-Pot Synthesis and Versatile Protonation Reaction

Thanh Dung Le,[a] Marie-Christine Weyland,[a] Yamna El-Harouch,[a] Damien Arquier,[a] Laure Vendier,[a] Karinne Miqueu,[b] Jean-Marc Sotiropoulos,[b] Stéphanie Bastin,[a] and Alain Igau*[a]

Keywords: Phosphanes / Formamidines / Protonation / Density functional calculations / Substituent effects

A straightforward synthesis of unprecedented *N*-phosphanylformamidines (phosfam), **3a**,**b** has been developed. The single-crystal X-ray study of **3a** revealed an *E*-formamidine stereoisomer. The structural parameters show a strong localization of the C1–N1 double bond in the formamidine pattern. Versatile protonation reactions with HCl on **3a** and **3b** are reported, leading to P–N cleavage vs. prototropy. Experimental studies and DFT calculations have evidenced that the imino nitrogen atom is the basic center of phosfams **3a** and **3b**. DFT calculations show that the isomers and rotamers of the *N*- and *P*-protonated forms of **8a**/**9a** and **8b**/**9b** are energetically close, which prevents conclusions being drawn on the existence of thermodynamic and/or kinetic products. The accessibility of the *anti* bonding PN orbital (σ^*_{P1N1}) is partly responsible for the cleavage of the PN bond in **8a**; **8b** possesses a less energetically accessible σ^*_{P1N1} orbital which is consistent with the preservation of the PN bond and the quantitative formation of the corresponding phosphonium compound **9b**·Cl.

Introduction

Formamidines are of special interest for general and synthetic organic chemistry.[1] Since the isolation of the first *N*-heterocyclic carbenes (NHC),[2] acyclic and cyclic compounds containing the formamidine functionality have been largely used as carbene precursors.[3] In the chemistry of neutral organic bases, formamidines belong to one of the most important families of strong bases.[4] Aiming at the preparation of new classes of P^{III}-functionalized phosphorus ligands, we were interested in preparing unprecedented *N*-phosphanylformamidine (phosfam) derivatives, $R_2'N–C(H)=N–PR_2$.[5,6] The bond between phosphorus and nitrogen in tervalent organophosphorus compounds is particularly susceptible to attack by Brönsted acids.[7] In aminophosphane chemistry, protonation reactions on the >P–N< unit take place under mild conditions with either cleavage or preservation of the phosphorus–nitrogen linkage.[8] Protonation reactions with preservation of the phosphorus–nitrogen linkage are believed to take place initially at the *P*-center. *P*-protonated phosphorus amides[9] as well as *P*-protonated phosphoramidite salts[10] have been prepared and characterized. To the best of our knowledge, an *N*-protonated isomer of a P^{III}–N amide unit has never been detected except when treating tetramethylguanidinyl P^{III} amides with HCl.[11]

If we refer to the results described in the literature on the protonation of aminophosphanes >P–N<[9–10] and (methyleneamino)phosphanes >P–N=C<[11] it is not possible to anticipate the privileged site of protonation of *N*-phosphanylformamidines **3a**,**b** and the thermodynamic stability of the corresponding protonated compounds.

Herein, we report the straightforward high-yield synthesis and the versatile protonation reaction of a new class of P^{III}-functionalized phosphorus derivatives, the *N*-phosphanylformamidines (phosfam) $iPr_2N–C(H)=N–PR_2$ **3a**,**b**. These studies were supported by quantum-chemical calculations.

Results and Discussion

N-Phosphanylformamidines **3a**,**b** were prepared in good yields in a one-pot procedure as single *E*-stereoisomers after treatment of the cyanamide derivative $iPr_2N–CN$ with successive additions of 1 equiv. of the hydridozirconocene complex **1**[12] and the corresponding chlorophosphanes R_2PCl (**2a**,**b**) (Scheme 1).

[a] Laboratoire de Chimie de Coordination, CNRS,
205 route de Narbonne, 31077 Toulouse Cedex 4, France
Fax: +33-5-61553003
E-mail: alain.igau@lcc-toulouse.fr
[b] IPREM CNRS 5254, Université de Pau & des Pays de l'Adour,
Avenue de l'Université, B. P. 1155, 64013 Pau cedex, France
E-mail: jean-marc.sotiro@univ-pau.fr

Supporting information for this article is available on the WWW under http://www.eurjic.org or from the author.

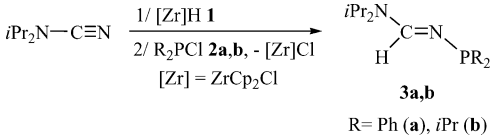

Scheme 1. Synthesis of *N*-phosphanylformamidines (phosfam) **3a**,**b**.

The composition and constitution of **3a**,**b** follow from mass analysis, IR, and ^{31}P, ^{1}H, ^{13}C, ^{15}N NMR spectra. The $^{3}J_{HP}$ [18.9 (**3a**) and 17.4 (**3b**) Hz] and $^{2}J_{CP}$ [52.7 (**3a**) and 47.9 (**3b**) Hz] coupling constants values, and the $^{1}J_{NP}$ coupling constant values of 44.6 (**3a**) and 39.4 (**3b**) Hz definitely confirmed the presence of the phosphanyl group $-PR_2$ attached to the formamidine fragment. X-ray quality crystals were obtained from a saturated pentane solution of **3a** at –5 °C, and the single-crystal X-ray study revealed an *E*-formamidine stereoisomer. As depicted in Figure 1, the compound exhibits pyramidal geometry at phosphorus with a classical covalent P–N bond length [1.697(2) Å] and a planar amino nitrogen atom iPr_2N-. The structural parameters of **3a** show a strong localization of the >C1=N1– double bond in the formamidine pattern. The C1–N1 bond length of 1.289(3) Å is in the range for carbon–nitrogen double bonds and there is a significant difference of 0.052 Å between the C1–N1 and C1–N2 bond lengths of the formamidine NC(H)N moiety.[13]

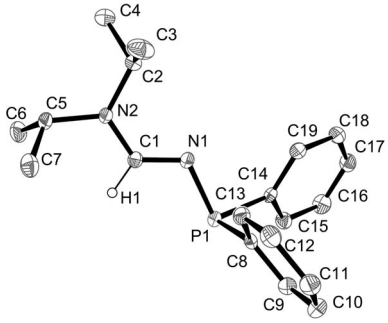

Figure 1. Molecular structure of **3a**. Hydrogen atoms have been omitted for clarity except for the formamidine hydrogen atom H1. Selected bond lengths [Å] and angles [°]: C1–N1 1.289(3), C1–N2 1.341(3), P1–N1 1.697(2), N2–C1–N1 123.5(2), C1–N1–P1 115.7(2).

In order to have a better insight into the geometrical and electronic structures of the phosfam derivatives, DFT calculations at the B3LYP/6-31G** level of theory were carried out on different formamidine derivatives iPr_2N–C(H)=NH (**4**) and iPr_2N–C(H)=N–PR_2 with R = H (**5**), Ph (**3a**), and *i*Pr (**3b**). As expected, for the phosfams **3a**,**b** and **5**, the *E* configuration corresponds to the most thermodynamically stable structure in which the imino nitrogen and phosphorus lone pairs are in a *trans* position.

The calculated geometrical parameters for **3a** are in good agreement with those recorded by X-ray crystallography (Table 1) and show that substitution of the proton on the imino nitrogen atom N1 of the formamidine **4** by a phosphanyl fragment $-PR_2$ leads only to weak changes. Moreover, the R substituents on the phosphorus atom in **3a**,**b** and **5** do not modify significantly the geometrical parameters of the formamidine skeleton iPr_2N–C(H)=N- (Table 1 and see Supporting Information).

Table 1. Selected bond lengths [Å] and angles [°] for formamidine **4** and *N*-phosphanylformamidines **5**, **3a**,**b**. NPA charges (qX).

X	**4**[a]	**5**[a]	**3a**[b]	**3a**[a]	**3b**[a]
C1–N1	1.286	1.292	1.289(3)	1.293	1.292
C1–N2	1.369	1.360	1.341(3)	1.358	1.362
P1–N1	/	1.741	1.697(2)	1.737	1.746
N2–C1–N1	123.82	124.05	123.5(2)	124.48	124.32
C1–N1–P1	109.45	114.77	115.7(2)	115.56	116.13
ΣP1	/	288.5	300.1	300.6	300.9
qN1	–0.77	–0.85	/	–0.89	–0.89
qN2	–0.48	–0.46	/	–0.46	–0.47
qP1	/	0.45	/	1.03	1.00
qC	0.26	0.29	/	0.30	0.29

[a] Calculated, see Supporting Information for details. [b] Observed, see Supporting Information for selected X-ray structure analysis data.

With regard to the molecular orbitals (MO), the HOMO and HOMO–1 in the *N*H-formamidine derivative **4** (Figure 2) are represented by the ($\pi_{C1N1} - n_{N2}$) and n_{N1} orbitals, respectively. For **3a** (Figure 2), the HOMO corresponds to the bonding combination of the phosphorus and nitrogen lone pairs ($n_{P1} + n_{N1}$) mixed with the σ_{P1N1} bond (*through-bond interaction*)[14] with an important weight on the phosphorus atom. Thus, the most striking changes between **4** and phosfam **3a** appear in the MO: the HOMO in **4**, is energetically more accessible than in **3a** but above all, the order of the first two orbitals is reversed with a decrease of the HOMO/HOMO–1 gap (1.1 eV for **4**, 0.6 eV for **3a**).

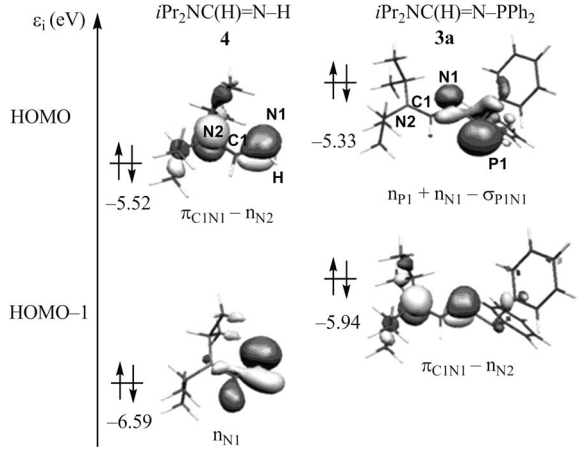

Figure 2. Molekel plots and energy levels (Kohn–Sham energies in eV) of the HOMO and HOMO–1 for **4** and **3a**.

In summary, DFT calculations confirmed that the lone pairs of the imino nitrogen and of the phosphorus atoms in **3a** are the two privileged binding sites. The additional binding site, the phosphanyl fragment $-PR_2$, in phosfam **3**[15] induces a drastic decrease of the HOMO/HOMO–1 gap and a change in the nature of the HOMO without modifying the structural parameters of the formamidine **4** to any great extent.

Natural Population Analysis coming from a NBO calculation shows that similar charges appear in **3** and **4**, the most negative charge being on the imino nitrogen. Protonation is a charge-controlled reaction, therefore, the imino nitrogen atom can be considered as the basic center of phosfams **3a** and **3b**. Consequently, as the first step of the protonation reaction with HCl, it seems reasonable to postulate the formation of the corresponding *N*-protonated formamidinium intermediates.

The protonation reaction of phosfam **3a** was investigated upon addition of HCl in solution in Et_2O. At 298 K in CH_2Cl_2, in the ^{31}P NMR spectrum of the reaction mixture, the initial chemical shift at δ = 54.3 ppm (**3a**) is replaced after addition of HCl by two broad signals at 31.7 and –17.6 ppm (**6**·Cl) (Scheme 2) which are resolved into two sharp doublets by exchanging the chloride for tetrafluoroborate to give **6**·BF_4 ($^1J_{PP}$ = 293 Hz).[16] The ^1H and ^{13}C NMR spectra of the reaction mixture showed the characteristic proton and carbon chemical shift of the formamidine framework >N–C(H)=N– of compound **6**·Cl and also evidenced the formation of the formamidinium product **7**·Cl in stoichiometric amount.

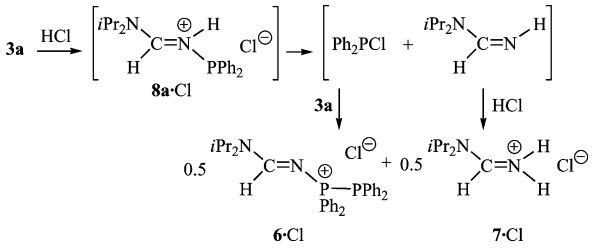

Scheme 2. Protonation reaction of phosfam **3a**.

In order to confirm the synthesis of **6**·Cl resulting from the in situ formation of Ph_2PCl in the protonation reaction of **3a** with HCl, **3a** was independently reacted with Ph_2PCl. Quantitative formation of **6**·Cl is observed (Scheme 3). Therefore, a protonation reaction on the methyleneaminophosphane **3a** with HCl takes place with cleavage of the =N–P< unit.

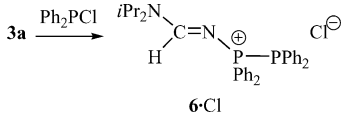

Scheme 3. Synthesis of the phosphanyl-phosphonium formamidine **6**·Cl.

The protonation reaction with HCl was then conducted on phosfam **3b**. After 4 h at room temperature, phosfam **3b** gave quantitatively the formamidine *P*H-phosphonium **9b**·Cl as the product of the reaction (Scheme 4). In the ^{31}P NMR spectrum, a signal appeared at δ = 50.4 ppm with a P–H coupling constant value ($^1J_{PH}$ = 459 Hz) characteristic of σ^4-PH compounds. The ^1H and ^{13}C NMR spectra of **9b**·Cl showed the presence of the proton at 9.06 ($^3J_{HP}$ = 21.9 Hz) ppm and the carbon at 162.6 ($^2J_{CP}$ = 2.5 Hz) ppm of the formamidine framework >N–C(H)=N–. Low-temperature NMR allowed us to characterize the *N*-protonated intermediate compound **8b**·Cl (Scheme 4), which was identified by the ^1H and ^{13}C chemical shifts of the formamidine skeleton >N–C(H)=N– at 7.51 (dd, $^3J_{HH}$ = 13.7 Hz, $^3J_{HP}$ = 6.1 Hz) and 156.6 (d; $^2J_{CP}$ = 45.1 Hz) ppm, respectively. The signal of the NH proton appeared at 11.24 (broad, $^3J_{HH}$ = 13.7 Hz) ppm. This assignment was confirmed by 2D ^{15}N NMR experiments which showed a chemical shift for the imino nitrogen atom at –258.4 ppm with N–H and N–P coupling constants of $^1J_{NH}$ 81.8 and $^1J_{NP}$ 56.5 Hz, respectively. At room temperature the *N*-protonated compound **8b**·Cl totally isomerizes to the isolated *P*-protonated phosphonium compound **9b**·Cl. The protonation reaction of **3b** with HCl occurs with preservation of the P–N bond to give the final isomerized product **9b**·Cl.

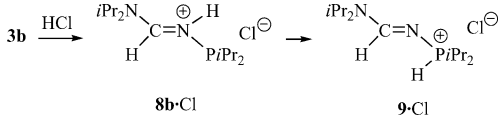

Scheme 4. Protonation reaction of phosfam **3b**.

Depending on the nature of the substituents R on the phosphorus atom, protonation reactions with HCl on phosfams **3** occur via either cleavage (R = Ph) or preservation (R = *i*Pr) of the P–N bond of the corresponding *N*-protonated compounds **8**·Cl, which has been observed and fully characterized for **8b**·Cl.

In order to obtain more insight on the protonation reactions of phosfams **3a**,**b**, DFT calculations were carried out. They show that in the gas phase the isomers of the *N*- and *P*-protonated forms of **8a**/**9a** and **8b**/**9b** are energetically close. These energy differences (<5 kcal/mol) between the isomers and rotamers are too weak to conclude on the existence of thermodynamic and/or kinetic products (see Supporting Information Figures S2 and S3). Since solvation can affect the relative stabilities of the isomeric structures, we carried out calculations using the PCM model.[15] We observed that the energy differences between the isomers remain weak with a slightly more thermodynamically stable structure corresponding to the *N*-protonated compounds, in agreement with the first experimentally postulated step. As previously observed for phosfams **3a**,**b**, the geometrical parameters of the formamidine skeleton $iPr_2N–C(H)=N–$ in the *N*- and *P*-protonated forms are not influenced by the substituents on the phosphorus atom (Table 2). The C1–N1 bond lengths for **8** and **9** are quasi similar. However, because of the presence of negative hyperconjugation between the imino nitrogen lone pair and the antiperiplanar σ^*_{P1H} orbital (ca. 11 kcal/mol: NBO calculation), the P1N1 bond lengths in the *P*-protonated forms **9** decreased drastically compared to the *N*-protonated forms **8** (Table 2).

To gain more insight into the origin of the PN bond splitting of **8a**, we evaluated the nature and the energy level of the molecular orbitals, more particularly the σ^*_{PN} one. We may notice that the LUMO and the LUMO+1 in **8a** are quasi of the same nature as in **8b** (Figure 3); they correspond to the π^*_{C1N1}–n_{N2} and σ^*_{P1N1} orbitals, respectively. However, their energy levels are substantially different. If

Table 2. Selected calculated[a] bond lengths [Å] and angles [°] for the *N*- and *P*-protonated forms **8a**,**b** and **9a**,**b**. NPA charges (qX).

X	8a	8b	9a	9b
C1–N1	1.327	1.329	1.318	1.317
C1–N2	1.316	1.316	1.327	1.325
P1–N1	1.817	1.810	1.634	1.631
N2–C1–N1	128.99	128.91	124.27	124.30
C1–N1–P1	121.24	121.38	122.71	124.56
ΣP1	301.9	302.8	/	/
qN1	–0.85	–0.86	–0.97	–0.98
qN2	–0.39	–0.39	–0.39	–0.39
qP1	1.09	1.06	1.64	1.62
qC	0.36	0.36	0.34	0.34

[a] See Supporting Information for details.

we specifically consider the two LUMO+1, their difference (0.6 eV) is significant; the energies of the orbitals are –3.23 eV for **8b** and –3.98 eV for **8a**, making the latter energetically more accessible.[17] On this basis, it is reasonable to propose that the accessibility of the *anti* bonding PN orbital (σ^*_{P1N1}) is partly responsible for the cleavage of the PN bond in **8a** followed by the in situ formation of Ph_2PCl. In contrast, **8b** possesses a less energetically accessible σ^*_{P1N1} orbital, which is consistent with the preservation of the PN bond and the quantitative formation of the phosphonium compound **9b**·Cl.

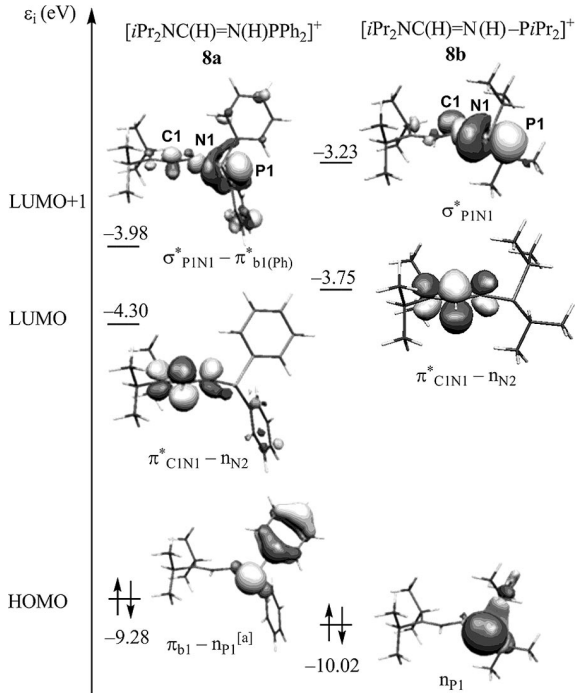

Figure 3. Molekel plots and energy levels (Kohn–Sham energies in eV) of the HOMO, LUMO, and LUMO+1 for **8a** and **8b**. [a]: the $n_P + \pi_{b1}$ orbital is at –10.64 eV.

Calculations in gas phase and in solution show that the energy barrier between the *N*- and *P*-protonated forms in the protonation reaction with phosfam **3b** is found to be high (Figure S4 in the Supporting Information: ca. 50–60 kcal/mol). Even if DFT calculations do not accurately model the barrier, this high value suggests that the isomerization process may involve an intermolecular rather than an intramolecular pathway.

Conclusions

In conclusion, we have developed a straightforward and high-yield synthesis of unprecedented *N*-phosphanylformamidine (phosfam) derivatives $R_2'N–C(H)=N–PR_2$. Experimental studies demonstrate that protonation reactions take place initially at the imino nitrogen center of the formamidine pattern, in agreement with PCM model DFT calculations. Surprisingly, replacing the substituent on the phosphorus atom from R = Ph to R = *i*Pr dramatically changes the course of the protonation reaction. The energy level of the molecular orbitals suggests that cleavage of the P–N unit in the *N*-protonated compound **8a** is induced by the accessibility of the antibonding PN orbital (σ^*_{P1N1}). Preservation of the phosphorus–nitrogen linkage upon protonation of **3b** is observed; the *N*-protonated compound **8b** isomerizes to form the corresponding PH phosphonium compound. Considering the high energy barrier, this formal prototropy process may involve a polymolecular rather than an intramolecular pathway. Studies on the reactivity of these new formamidines are underway. Since the electronic and steric properties of the phosphane and the imino nitrogen centers can be finely and easily tuned, studies to evaluate the potential uses of these ligands in catalysis are under active investigation.

Experimental Section

General Information: All reactions were conducted under an inert atmosphere of dry argon using standard Schlenk-line techniques. Chemicals were treated as follows: pentane and CH_2Cl_2 distilled from CaH_2. $CDCl_3$ distilled from P_2O_5; C_6D_6, CD_2Cl_2 (Euriso-top) and other solvents stored on 4-Å molecular sieves. Solvents were degassed by standard methods before use. Chlorodiphenylphosphane (97%) was obtained from ALFA AESAR and distilled prior to use. All other commercial chemicals were from Aldrich (*N*,*N*-diisopropylcyanamide, 97% and hydrochloric acid solution 1 M in diethyl ether), Acros (chlorodiisopropylphosphane, 96%), and Strem [bis(cyclopentadienyl)zirconium dichloride, 99%] and were used as received. $[Cp_2ZrHCl]_n$ was prepared following the procedure reported by Buchwald et al.[12a]

NMR spectra were recorded with Bruker AV 500, AV 400, AV 300, or AC200 spectrometers. Chemical shifts for ^1H and ^{13}C are referenced to residual solvent resonances used as an internal standard and reported relative to $SiMe_4$. ^{31}P and ^{15}N NMR chemical shifts are reported relative to external aqueous 85% H_3PO_4 (^{31}P) and CH_3NO_2 (^{15}N), respectively. All the ^1H and ^{13}C signals were assigned on the basis of chemical shifts, spin-spin coupling constants, splitting patterns and signal intensities, and by using 2D experiments such as $^1H–^1H$ COSY45, $^1H–^{13}C$ HMQC, and $^1H–^{13}C$ HMBC experiments. All spectra were recorded at ambient probe temperature unless stated otherwise. Crude reaction mixtures were controlled by NMR in CH_2Cl_2 with a sealed tube of [D_8]toluene as a reference. All compounds were then fully characterized in the deuterated solvent stated in the experimental part. Infrared spectra

were performed in solution (KBr windows) with a Perkin–Elmer GX 2000 spectrometer. Mass spectra were recorded with a TSQ7000 Thermo Electron (EI) and a Q Trap (ES–MS) mass spectrometer. Melting points were obtained using an Electrothermal Digital Melting Point apparatus and are uncorrected. Elemental analyses were carried out by the "Service d'Analyse du Laboratoire de Chimie de Coordination" in Toulouse.

Representative Experimental Procedure for the Preparation of *N*-Phosphanylformamidines *i*Pr$_2$NC(H)=N–PR$_2$ (3a,b): A solution of *i*Pr$_2$NCN (0.986 g, 7.814 mmol) in CH_2Cl_2 (5 mL) was added to a suspension of $[Cp_2Zr(H)Cl]_n$ (**1**, 2.015 g, 7.814 mmol) in CH_2Cl_2 (15 mL) in a Schlenk flask under argon. The suspension was stirred for 1 h until a pale yellow solution was obtained. R_2PCl (7.814 mmol) was then slowly added via syringe, resulting in a colorless solution. The solvent was removed by oil pump vacuum to give a white residue that was extracted using pentane (3 × 20 mL) to give **3a** in 91% yield (2.221 g, 7.111 mmol) and **3b** in 85% yield (1.622 g, 6.642 mmol).

***i*Pr$_2$NC(H)=N–PPh$_2$ (3a):** IR (KBr, THF): $\tilde{\nu}$ = 1612 cm^{-1} (C=N). $^{31}P\{^1H\}$ NMR (121.5 MHz, CD_2Cl_2, 25 °C): δ = 54.3 ppm. ^1H NMR (300.1 MHz, CD_2Cl_2, 25 °C): δ = 8.14 (d, $^3J_{H,P}$ = 18.9 Hz, 1 H, C*H*=N), 7.60–7.34 (m, 10 H, H_{Ph}), 4.85 [sept, ^3J(H,H) = 5.7 Hz, 1 H, C*H*CH$_3$], 3.66 (sept, $^3J_{H,H}$ = 5.7 Hz, 1 H, C*H*CH$_3$), 1.38 (d, $^3J_{H,H}$ = 5.7 Hz, 6 H, CHC*H*$_3$), 1.31 (d, $^3J_{H,H}$ = 5.7 Hz, 6 H, CHC*H*$_3$) ppm. $^{13}C\{^1H\}$ NMR (75.5 MHz, CD_2Cl_2, 25 °C): δ = 158.6 (d, $^2J_{C,P}$ = 52.7 Hz, *C*H=N), 145.0 (d, $^1J_{C,P}$ = 12.3 Hz, C_{Ph}), 130.7 (d, $J_{C,P}$ = 19.7 Hz, *C*H$_{Ph}$), 128.0 (s, *C*H$_{Ph}$), 127.9 (d, $J_{C,P}$ = 1.8 Hz, *C*H$_{Ph}$), 47.0 (s, N*C*HCH$_3$), 45.2 (s, N*C*HCH$_3$), 23.6 (s, NCH*C*H$_3$), 19.9 (s, NCH*C*H$_3$) ppm. ^{15}N NMR (40.6 MHz, [D$_8$]-toluene, 25 °C): δ = –182.2 ($^1J_{N,P}$ = 44.6 Hz, C=*N*–P), –243.9 (*Ni*Pr$_2$) ppm. EI MS: *m*/*z* (%) = 312 (1) [M$^+$], 220 (100) [M$^+$ – CH$_3$ – Ph]. $C_{19}H_{25}N_2P$ (312.1755): calcd. C 73.05, H 8.07, N 8.97; found C 73.16, H 8.15, N 8.85.

***i*Pr$_2$NC(H)=N–P*i*Pr$_2$ (3b):** IR (KBr, THF): $\tilde{\nu}$ = 1606 cm^{-1} (C=N). $^{31}P\{^1H\}$ NMR (161.9 MHz, CD_2Cl_2, 25 °C): δ = 90.0 ppm. ^1H NMR (400.1 MHz, CD_2Cl_2, 25 °C): δ = 7.88 (d, $^3J_{H,P}$ = 17.4 Hz, 1 H, C*H*=N), 4.43 (br. m, 1 H, NC*H*CH$_3$), 3.52 (br. m, 1 H, NC*H*CH$_3$), 1.66 (sept, $^3J_{H,H}$ = 6.9 Hz, 2 H, PC*H*CH$_3$), 1.21 (d, $^3J_{H,H}$ = 6.9 Hz, 6 H, NCHC*H*$_3$), 1.19 (d, $^3J_{H,H}$ = 6.9 Hz, 6 H, NCHC*H*$_3$), 0.97 (dd, $^3J_{H,P}$ = 11.9, $^3J_{H,H}$ = 6.9 Hz, 12 H, PCHC*H*$_3$) ppm. $^{13}C\{^1H\}$ NMR (100.6 MHz, CD_2Cl_2, 25 °C): δ = 158.2 (d, $^2J_{C,P}$ = 47.9 Hz, *C*H=N), 47.2 (s, N*C*HCH$_3$), 45.1 (s, N*C*HCH$_3$), 26.6 (d, $^1J_{C,P}$ = 9.9 Hz, P*C*HCH$_3$), 23.7 (s, NCH*C*H$_3$), 20.1 (s, NCH*C*H3), 18.9 (d, $^2J_{C,P}$ = 19.8 Hz, PCH*C*H$_3$), 17.6 (d, $^2J_{C,P}$ = 7.8 Hz, PCH*C*H$_3$) ppm. ^{15}N NMR (40.6 MHz, [D$_8$]toluene): δ = –177.8 ($^1J_{N,P}$ = 39.4 Hz, C=*N*–P), –240.1 (*Ni*Pr$_2$) ppm. EI MS: *m*/*z* (%) = 244 (1) [M$^+$], 201 (47) [M$^+$ – *i*Pr]. $C_{13}H_{29}N_2P$ (244.2068): calcd. C 63.90, H 11.96, N 11.46; found C 64.12, H 12.08, N 11.22.

Protonation Reaction on *i*Pr$_2$NC(H)=N–PPh$_2$ (3a): To a solution of *N*-phosphanylformamidine **3a** (0.156 g, 0.500 mmol) in CH_2Cl_2 (8 mL) hydrochloric acid (0.500 mL, 1 M in diethyl ether) was added dropwise at –78 °C. The reaction mixture was warmed to room temperature and stirred for 10 min. The solvent was removed by oil pump vacuum to give a white residue constituted of a mixture of **6**·Cl and **7**·Cl as the sole products of the reaction according to NMR analysis. These compounds were not isolated, they were independently prepared as described below in order to confirm their composition and constitution.

Addition of Ph$_2$PCl on *i*Pr$_2$NC(H)=N–PPh$_2$ (3a): A Schlenk flask was charged with *i*Pr$_2$NC(H)=NPPh$_2$ (**3a**, 0.151 g, 0.480 mmol), Ph_2PCl (**2a**, 0.106 g, 0.480 mmol), and CH_2Cl_2 (5 mL). The mixture was stirred for 5 min. The solvent was removed by oil pump vacuum to give **6**·Cl in quantitative yield as a white residue (0.256 g, 0.480 mmol). Compound **6**·Cl was characterized by NMR without any further treatment. ^{31}P NMR (81.0 MHz, $CDCl_3$, 25 °C): δ = 31.7 (d, $^1J_{P,P}$ = 282.5 Hz), –17.6 (d, $^1J_{P,P}$ = 282.5 Hz) ppm. ^1H NMR (200.1 MHz, $CDCl_3$, 25 °C): δ = 7.58–7.03 (m, 21 H, H_{Ph} and C*H*=N), 4.37 (sept, $^3J_{H,H}$ = 6.8 Hz, 1 H, NC*H*CH$_3$), 3.54 (sept, $^3J_{H,H}$ = 6.7 Hz, 1 H, NC*H*CH$_3$), 1.12 (d, $^3J_{H,H}$ = 6.8 Hz, 6 H, NCHC*H*$_3$), 0.92 (d, $^3J_{H,H}$ = 6.7 Hz, 6 H, NCHC*H*$_3$) ppm. $^{13}C\{^1H\}$ NMR (50.3 MHz, $CDCl_3$, 25 °C): δ = 156.5 (d, $^2J_{C,P}$ = 3.4 Hz, *C*H=N), 135.1 (d, $^1J_{C,P}$ = 7.0 Hz, *i*C$_{Ph}$), 134.7 (d, $^1J_{C,P}$ = 10.4 Hz, *i*C$_{Ph}$), 134.5 (s, C$_{Ph}$), 134.2 (s, C$_{Ph}$), 131.9 (d, $J_{C,P}$ = 8.8 Hz, C$_{Ph}$), 131.3 (s, C$_{Ph}$), 129.7 (d, J = 11.8 Hz, C$_{Ph}$), 129.3 (d, $J_{C,P}$ = 7.3 Hz, C$_{Ph}$), 50.1 (s, N*C*HCH$_3$), 47.8 (s, N*C*HCH$_3$), 23.1 (s, NCH*C*H$_3$), 19.3 (s, NCH*C*H$_3$) ppm. ^{15}N NMR (50.7 MHz, [D$_8$]toluene, 25 °C): δ = –210.0 (N*i*Pr$_2$), –244.0 ($^1J_{N,P}$ = 51.0 Hz, C=N–P) ppm.

Synthesis of the Formamidinium 7·Cl: A solution of *i*Pr$_2$NCN (0.095 g, 0.750 mmol) in CH_2Cl_2 (5 mL) was added to a suspension of $[Cp_2Zr(H)Cl]_n$ (**1**, 0.193 g, 0.750 mmol) in CH_2Cl_2 (15 mL) in a Schlenk flask under argon. The suspension was stirred for 1 h until a pale yellow solution was obtained. A solution of hydrochloric acid (1 M in diethyl ether) (0.750 mL, 0.750 mmol) in 5 mL of CH_2Cl_2 was then added at 0 °C. The reaction mixture was stirred for 1 h at room temperature. The solvent was removed by oil pump vacuum and the residue obtained was washed with THF (3 × 10 mL) to give **7**·Cl as a white powder in 90% yield (0.111 g, 0.675 mmol); m.p. 280 °C. IR (KBr, $CHCl_3$): $\tilde{\nu}$ = 1695 cm^{-1} (C=N). ^1H NMR (400.1, $CDCl_3$, 25 °C): δ = 10.25 (br. s, 1 H, NH_2), 9.95 (d, $^3J_{H,H}$ = 14.1 Hz, 1 H, NH_2), 7.56 (dd, $^3J_{H,H}$ = 14.1, $^3J_{H,H}$ = 6.3 Hz, 1 H, CH=N), 4.78 (sept, $^3J_{H,H}$ = 6.8 Hz, 1 H, NC*H*CH$_3$), 3.80 (sept, $^3J_{H,H}$ = 6.8 Hz, 1 H, NC*H*CH$_3$), 1.35 (d, $^3J_{H,H}$ = 6.8 Hz, 6 H, NCHC*H*$_3$), 1.34 (d, $^3J_{H,H}$ = 6.8 Hz, 6 H, NCHC*H*$_3$) ppm. $^{13}C\{^1H\}$ NMR (100.6, $CDCl_3$): δ = 151.4 (s, CH=N), 50.0 (s, CHCH$_3$), 48.5 (s, CHCH$_3$), 24.3 (s, CHCH$_3$), 19.9 (s, CH CH$_3$) ppm. ESI MS: *m*/*z* (%) = 129 [M – Cl]$^+$.

Protonation Reaction on *i*Pr$_2$NC(H)=N–P*i*Pr$_2$ (3b). Synthesis of *N*-Phosphonioformamidine Chloride [*i*Pr$_2$NC(H)=N–P(H)*i*Pr$_2$]Cl (9b·Cl): To a solution of *N*-phosphanylformamidine **3b** (0.122 g, 0.500 mmol) in CH_2Cl_2 (8 mL) hydrochloric acid (0.500 mL, 1 M in diethyl ether) was added dropwise at –78 °C. The reaction mixture was warmed to room temperature and stirred for 10 min. The solvent was removed by oil pump vacuum to give a white residue that was washed using pentane (3 × 20 mL) to give **9b**·Cl. Yield: 75% (0.105 g, 0.375 mmol). IR (KBr, THF): $\tilde{\nu}$ = 1603 cm^{-1} (C=N). ^{31}P NMR (161.9 MHz, $CDCl_3$, 25 °C): δ = 50.4 (d; $^1J_{H,P}$ = 458.8 Hz, *P*H) ppm. ^1H NMR (400.1 MHz, $CDCl_3$, 25 °C): δ = 9.06 (d; $^3J_{H,P}$ = 21.9 Hz, 1 H, C*H*=N), 7.75 (d; $^1J_{H,P}$ = 458.8 Hz, 1 H, PH), 4.24 (sept, $^3J_{H,H}$ = 6.8 Hz, 1 H, NC*H*CH$_3$), 3.65 (sept, $^3J_{H,H}$ = 6.8 Hz, 1 H, NC*H*CH$_3$), 2.43 (br. m, 1 H, PC*H*CH$_3$), 2.31 (br. m, 1 H, PC*H*CH$_3$), 1.22 (d, $^3J_{H,H}$ = 6.8 Hz, 6 H, NCHC*H*$_3$), 1.14 (dd, $^3J_{H,H}$ = 6.4, $^3J_{H,P}$ = 2.0 Hz, 12 H, PCHC*H*$_3$), 1.11 (d, $^3J_{H,H}$ = 6.8 Hz, 6 H, NCHC*H*$_3$) ppm. $^{13}C\{^1H\}$ NMR (100.6 MHz, $CDCl_3$, 25 °C): δ = 162.6 (d; $^2J_{C,P}$ = 2.5 Hz, H*C*=N), 50.6 (s; N*C*HCH$_3$), 46.8 (s; N*C*HCH$_3$), 23.4 (s; NCH*C*H$_3$), 22.8 (d; $^1J_{C,P}$ = 63.2 Hz, P*C*HCH$_3$), 19.8 (s; NCH*C*H$_3$), 16.5 (d; $^2J_{C,P}$ = 2.0 Hz, PCH*C*H$_3$), 15.6 (d; $^2J_{C,P}$ = 3.7 Hz, PCH*C*H$_3$) ppm. ^{15}N NMR (40.6 MHz, [D$_8$]toluene): δ = –219.0 (*N* *i*Pr$_2$), –248.1 ($^1J_{N,P}$ = 38.8 Hz, C=*N*–P) ppm.

Protonation Reaction on *i*Pr$_2$NC(H)=N–P*i*Pr$_2$ (3b): Identification of [*i*Pr$_2$NC(H)=N(H)–P*i*Pr$_2$]Cl, **8b**·Cl by low-temperature NMR spectroscopy: ^{31}P NMR (161.9 MHz, CD_2Cl_2, 0 °C): δ = 98.9 ppm. ^1H NMR (400.1 MHz, CD_2Cl_2, 0 °C): δ = 11.24 (br. d, $^3J_{H,H}$ = 13.7 Hz, 1 H, N*H*), 7.51 (dd, $^3J_{H,H}$ = 13.7, $^3J_{H,P}$ = 6.1 Hz, 1 H,

C*H*=N), 3.79 (sept, $^3J_{H,H}$ = 6.8 Hz, 1 H, NC*H*CH_3), 3.15 (sept, $^3J_{H,H}$ = 6.5 Hz, 1 H, NC*H*CH_3), 2.48 (br. m, 1 H, PC*H*CH_3), 2.39 (br. m, 1 H, PC*H*CH_3), 1.24 (d, $^3J_{H,H}$ = 6.8 Hz, 6 H, NCHC*H*$_3$), 1.17 (d, $^3J_{H,H}$ = 6.5 Hz, 6 H, NCHC*H*$_3$), 1.00 (dd, $^3J_{H,H}$ = 7.1, $^3J_{H,P}$ = 17.3 Hz, 12 H, PCHC*H*$_3$) ppm. $^{13}C\{^1H\}$ NMR (100.6, CD_2Cl_2, 0 °C): δ = 156.6 (d, $^2J_{C,P}$ = 45.1 Hz, H*C*=N), 51.9 (s, N*C*HCH$_3$), 48.2 (s, N*C*HCH$_3$), 25.8 (d, $^1J_{C,P}$ = 11.2 Hz, P*C*HCH$_3$), 24.3 (s, NCH*C*H$_3$), 21.6 (s, NCH*C*H$_3$), 18.9 (d, $^2J_{CP}$ = 7.2 Hz, PCH*C*H$_3$), 18.6 (d, $^2J_{CP}$ = 20.6 Hz, PCH*C*H$_3$) ppm. ^{15}N NMR ([D$_8$]toluene, 40.6 MHz, 0 °C): δ = –220.0 (*Ni*Pr$_2$), –258.4 [$J_{N,H}$ = 81.8, J_{NP} = 56.5 Hz, C=*N*(H)–P] ppm.

X-ray Crystal Structure Determination of Compound 3a: Crystallographic data were collected at low temperature (180 K) with a Xcalibur Oxford-Diffraction diffractometer using graphite-monochromated Mo-K_α radiation (λ = 0.71073 Å) and equipped with an Oxford Cryosystems Cryostream Cooler Device. The final unit cell parameters were obtained by means of least-squares refinement performed on a set of 2310 well-measured reflections. The structure was solved by Direct Methods using SIR92,[18] and refined by means of least-squares procedures on F^2 with the aid of the program SHELXL97[19] included in the software package WinGX version 1.63.[20] The Atomic Scattering Factors were taken from International tables for X-ray crystallography.[21] All hydrogen atoms were geometrically placed and refined by using a riding model.

Crystallographic Data for 3a: Colorless platelet (0.17 × 0.17 × 0.05 mm), $C_{19}H_{25}N_2P$, M = 312.38, triclinic, a = 7.4702(14) Å, b = 9.915(3) Å, c = 13.169(4) Å, α = 104.57(2)°, β = 102.56 (2)°, γ = 97.098(18) , V = 904.9(4) Å^3, T = 180 K, space group P-1 (no. 2), Z = 2, μ(Mo-K_α) = 0.151 mm^{-1}, 6498 reflections measured, 3425 unique (Rint = 0.0565) which were used in all calculations, R = 0.0578 (wR = 0.1259) for 3425 reflections with [$I > 2\sigma(I)$], GOF = 1.088. Semi-empirical absorption corrections were performed.[22] All non-hydrogen atoms were anisotropically refined, and in the last cycles of refinement a weighting scheme was used, where weights were calculated from the following formula: $w = 1/[\sigma^2(F_o^2) + (aP)^2 + bP]$ where $P = (F_o^2 + 2F_c^2)/3$. The drawing of the molecule was performed with the program ORTEP32[23] with 30% probability displacement ellipsoids for non-hydrogen atoms.

CCDC-614899 contains the supplementary crystallographic data for his paper. These data can be obtained free of charge from the Cambridge Crystallographic Data Center via www.ccdc.cam.ac.uk/data_request/cif.

Computational Details: Calculations were performed with the Gaussian 98 and 03 programs,[24,25] using the density functional method.[26] The hybrid exchange functional B3LYP in conjunction with the 6-31G** basis set was used. B3LYP[27] is a three-parameter functional developed by Becke which combines the Becke gradient-corrected exchange functional and the Lee–Yang–Parr and Vosko–Wilk–Nusair correlation functionals with part of the exact HF exchange energy. The optimized structures were confirmed as true minima on the potential energy through vibrational analysis. The frequencies were calculated with analytical second derivatives. All total energies were zero-point energy (ZPE) and temperature-corrected using unscaled density functional frequencies. Natural bond orbital (NBO) analysis was used to calculate the natural charges.[28] Molecular orbitals have been plotted with the Molekel package.[29] Solvent effect calculations were performed with the PCM[30] model implemented in Gaussian 03. The total energy and total free energy were evaluated from single-point PCM calculations on the gas phase optimized geometries at the same level of theory. CH_2Cl_2 was used as the solvent as in the experimental work.

The transition state was calculated using the STQN method implemented in Gaussian (opt = QST3). The connection between the transition state and the corresponding minima was confirmed by IRC calculations.

Supporting Information (see also the footnote on the first page of this article): Selected crystallographic data for **3a** and detailed calculated data for all compounds.

Acknowledgments

We thank the Institut du Developpement de Ressources en Informatique Scientifique administered by the CNRS, for the calculation facilities. Y. E.-H. is grateful to the Ministère de la Recherche for a doctoral fellowship. D. A. thanks the European Community for a post-doctoral fellowship (FSE).

[1] T. M. Krygowski, K. Wozniak, in *The Chemistry of Amidines and Imidates* (Eds.: S. Patai, Z. Rappoport), John Wiley & Sons, Chichester, **1991**.
[2] A. J. Arduengo III, R. L. Harlow, M. Kline, *J. Am. Chem. Soc.* **1991**, *113*, 361–363.
[3] a) Y. Ishida, B. Donnadieu, G. Bertrand, *PNAS* **2006**, *103*, 13585–13588; b) K. E. Krahulic, G. D. Enright, M. Parvez, R. Roesler, *J. Am. Chem. Soc.* **2005**, *127*, 4142–4143; c) E. Despagnet-Ayoub, R. H. Grubbs, *J. Am. Chem. Soc.* **2004**, *126*, 10198–10199.
[4] E. D. Raczynska, P.-C. Maria, J.-F. Gal, M. Decouzon, *J. Org. Chem.* **1992**, *27*, 5730–5735.
[5] It is important to note that *N*-phosphanyl amidines (R′$_2$N) R′′C=N–PR$_2$ (R′′ ≠ H) have been already described in the literature[6] but their method of preparation can not be extended to the synthesis of the corresponding formamidine derivatives.
[6] a) U. Scholz, M. Noltemeyer, H. W. Roesky, *Z. Naturforsch., Teil B* **1988**, *43*, 937–940; b) V. Chandrasekhar, T. Chivers, S. S. Kumaravel, A. Meetsma, J. C. Van de Grampel, *Inorg. Chem.* **1991**, *30*, 3402–3407; c) E. Rivard, A. J. Lough, T. Chivers, I. Manners, *Inorg. Chem.* **2004**, *43*, 802–811.
[7] O. Dahl in *The Chemistry of Organophosphorus Compounds* (Ed.: F. R. Hartley), John Wiley & Sons, Chichester, **1996**, vol. 4, pp. 1–45 and references cited therein.
[8] a) O. Dahl, *Tetrahedron Lett.* **1982**, *23*, 1493–1496; G. S. Harris, *J. Chem. Soc.* **1958**, 512; b) A. B. Burg, P. J. Slota, *J. Am. Chem. Soc.* **1958**, *80*, 1107–1109; c) K. Issleib, W. Seidel, *Chem. Ber.* **1959**, *92*, 2681–2694; d) K. Drewelies, H. P. Latscha, *Angew. Chem. Int. Ed. Engl.* **1982**, *21*, 638–639.
[9] a) E. E. Nifant'ev, M. K. Gratchev, S. Yu. Burmistrov, *Chem. Rev.* **2000**, *100*, 3755–3799; b) E. E. Nifant'ev, M. K. Gratchev, S. Yu. Burmistrov, L. K. Vasyanina, M. Y. Antipin, Y. T. Struchkov, *Tetrahedron* **1991**, *47*, 9839–9860.
[10] a) E. J. Nurminen, H. Lönnberg, *J. Phys. Org. Chem.* **2004**, *17*, 1–17; b) E. J. Nurminen, J. K. Mattinen, H. Lönnberg, *J. Chem. Soc. Perkin Trans. 2* **2000**, 2238–2240.
[11] V. Plack, J. Münchenberg, H. Thönnessen, P. G. Jones, R. Schmutzler, *Eur. J. Inorg. Chem.* **1998**, 865–875.
[12] a) S. L. Buchwald, S. J. LaMaire, R. B. Nielsen, B. T. Watson, S. M. King, *Tetrahedron Lett.* **1987**, *28*, 3895–3898; b) A. Igau in *Catalytic Heterofunctionalization* (Eds.: A. Togni, H. Grützmacher), Wiley-VCH, Weinheim, **2001**, pp. 253–282.
[13] C–N bonds in organic formamidine derivatives have only a partial double bond, see: a) T. M. Krygowski, K. Wozniak, in *The Chemistry of Amidines and Imidates* (Eds.: S. Patai, Z. Rappoport), John Wiley & Sons, Chichester, **1991**, p. 101–147; b) A. G. Orpen, L. Brammer, F. H. Allen, O. Kennard, D. G. Watson, R. Taylor, in *Structure Correlation* (Eds.: H.-B. Bürgi, J. D. Dunitz), VCH, Weinheim, **1994**, vol. 2, pp. 770–774.
[14] R. Hoffmann, *Acc. Chem. Res.* **1971**, *4*, 1–9.

[15] For DFT calculations on **3b** see Supporting Information.
[16] For $^1J_{PP}$ range values in phosphanyl-phosphonium derivatives see for example: a) N. Burford, C. A. Dyker, A. Decken, *Angew. Chem. Int. Ed.* **2005**, *44*, 2364–2367; b) N. Burford, D. E. Herbert, P. Ragogna, R. McDonald, M. J. Ferguson, *J. Am. Chem. Soc.* **2004**, *126*, 17067–17073; c) A. H. Cowley, R. A. Kemp, *Chem. Rev.* **1985**, *85*, 367–382; d) D. Gudat, *Eur. J. Inorg. Chem.* **1998**, 1087–1094 and references cited therein.
[17] DFT calculations with the Cl^- counterion (optimization of the geometry of **8** in the presence of Cl^-: **8·Cl**) have also been carried out. The geometrical parameters are quasi unchanged and the energy difference between the σ^*_{P1N1} orbitals in **8a·Cl** and **8b·Cl** is intensified (0.05 eV for **8b·Cl** and –1.05 eV for **8a·Cl**, energy difference: 1.1 eV): see Figure S1 in SI.
[18] A. Altomare, G. Cascarano, C. Giacovazzo, A. Guagliardi, *SIR92*, A Program for Crystal Structure Solution, *J. Appl. Crystallogr.* **1993**, *26*, 343–350.
[19] G. M. Sheldrick, *SHELX97* (includes SHELXS97, SHELXL97, CIFTAB), Programs for Crystal Structure Analysis (release 97-2), Universität Göttingen, Göttingen, Germany, **1998**.
[20] L. J. Farrugia, *WINGX-1.63*, Integrated System of Windows Programs for the Solution, Refinement and Analysis of Single Crystal X-ray Diffraction Data, *J. Appl. Crystallogr.* **1999**, *32*, 837–838.
[21] *International Tables for X-ray Crystallography*, Kynoch Press, Birmingham, England, **1974**, vol. 4.
[22] R. H. Blessing, *Acta Crystallogr., Sect. A* **1995**, *51*, 33–58.
[23] L. J. Farrugia, *ORTEP32 for Windows*, *J. Appl. Crystallogr.* **1997**, *30*, 565.
[24] M. J. Frisch, G. W. Trucks, H. B. Schlegel, G. E. Scuseria, M. A. Robb, J. R. Cheeseman, V. G. Zakrzewski, J. A. Montgomery, R. E. Stratman, J. C. Burant, S. Dapprich, J. M. Millam, A. D. Daniels, K. N. Kudin, M. C. Strain, O. Farkas, J. Tomasi, V. Barone, M. Cossi, R. Cammi, B. Mennucci, C. Pomelli, C. Adamo, S. Clifford, J. Ochterski, G. A. Petersson, P. Y. Ayala, Q. Cui, K. Morokuma, D. K. Malick, A. D. K. Rabuck, K. Raghavachari, J. B. Foresman, J. Cioslowswi, J. V. Ortiz, A. G. Baboul, B. B. Stefanov, G. Liu, A. Liashenko, P. Piskorz, I. Komaromi, R. Gomperts, R. Martin, D. J. Fox, T. Keith, M. A. Al-Laham, C. Y. Peng, A. Nanayakkara, C. Gonzalez, M. Challacombe, P. M. W. Gill, B. Johnson, W. Chen, M. W. Wong, J. L. Andres, M. Head-Gordon, E. S. Replogle, J. A. Pople, *Gaussian 98*, Revision A.7, Gaussian, Inc., Pittsburgh PA, **2001** (A.11.1) or **2003** (A.11.3).
[25] W. J. Hehre, L. Radom, P. v. R. Schleyer, J. A. Pople, *Ab initio Molecular Orbital Theory*, John Wiley & Sons, New York, **1986**.
[26] R. G. Parr, W. Yang, *Functional Theory of Atoms and Molecules* (Eds.: R. Breslow, J. B. Goodenough), Oxford University Press, New York, **1989**.
[27] a) A. D. Becke, *Phys. Rev. A* **1988**, *38*, 3098–3100; b) A. D. Becke, *J. Chem. Phys.* **1993**, *98*, 5648–5652; c) C. Lee, W. Yang, R. G. Parr, *Phys. Rev. B* **1988**, *37*, 785–789.
[28] a) A. E. Reed, L. A. Curtiss, F. Weinhold, *Chem. Rev.* **1988**, *88*, 899–926; b) J. P. Foster, F. Weinhold, *J. Am. Chem. Soc.* **1980**, *102*, 7211–7218.
[29] a) P. Flükiger, H. P. Lüthi, S. Portmann, J. Weber, *Molekel 4.3*, Swiss Center for Scientific Computing, Manno, Switzerland, **2000**–**2002**; b) S. Portmann, H. P. Lüthi, *Molekel: An Interactive Molecular Graphics Tool*, *Chimia* **2000**, *54*, 766–770.
[30] a) S. Miertus, J. Tomasi, *Chem. Phys.* **1982**, *65*, 239–245; b) S. Miertus, E. Scrocco, J. Tomasi, *Chem. Phys.* **1981**, *55*, 117–129; c) M. Cossi, V. Barone, R. Cammi, J. Tomasi, *Chem. Phys. Lett.* **1996**, *255*, 327–335.

Received: December 3, 2007
Published Online: April 21, 2008

